Maja Vujović, Venkatesan Ragavendran, Biljana Arsić*, Emilija Kostić, Milan Mladenović

DFT calculations as an efficient tool for prediction of Raman and infra-red spectra and activities of newly synthesized cathinones

Abstract: Initially made for medical treatment for Parkinsonism, obesity, and depression, cathinones have become illegal drugs for the "recreational use". The mechanism of action of synthetic cathinones consists of the inhibition of monoamine transporters. DFT (Density Functional Theory) calculations on the selected cathinones (3-FMC, 4-FMC, 4-MMC, Buphedrone, Butylone, Ethylone, MDPV, Methcathinone, and Methylone) were performed using B3LYP level of the Gaussian 09 program suite. The unscaled B3LYP/6–31G vibrational wavenumbers are in general larger than the experimental values, so the use of selective scaling was necessary. The calculated spectra of selected cathinones are in good correlation with the experimental spectra which demonstrates that DFT is a good tool for the prediction of spectra of newly synthesized and insufficiently experimentally characterised cathinones. Also, HOMO-LUMO (Highest Occupied Molecular Orbital-Lowest Unoccupied Molecular Orbital) analysis shows that 3-FMC possesses the minimum energy gap of 3.386 eV, and the molecule 4-FMC possesses the maximum energy gap of 4.205 eV among the investigated cathinones. It indicates that 3-FMC would be highly reactive among all the cathinones under investigation.

Keywords: cathinones; DFT; spectra; reactivity.

*Corresponding author: Biljana Arsić, University of Niš, Faculty of Sciences and Mathematics, Department of Mathematics, Višegradska 33, 18000 Niš, Republic of Serbia, E-mail: ba432@ymail.com
Maja Vujović, Emilija Kostić, University of Niš, Faculty of Medicine, Department of Pharmacy, Bulevar Dr Zorana Đinđića 81, 18000 Niš, Republic of Serbia
Venkatesan Ragavendran, Department of Physics, Sri Chandrasekharendra Saraswathi Viswa Mahavidyalaya, Kanchipuram, 631561, Tamilnadu, India
Milan Mladenović, Kragujevac Center for Computational Biochemistry, Faculty of Science, University of Kragujevac, Radoja Domanovića 12, 34000 Kragujevac, P.O. Box 60, Republic of Serbia

1 Introduction

The illegal drugs problem has reached an epidemic level with the increased number of registered users and deaths caused by overdoses, with the causes of this phenomenon being numerous.

Usually, illegal drugs are divided into synthetic cannabinoids, synthetic cathinones, phenethylamines, arylcyclohexylamines, and tryptamines [1]. Synthetic cathinones [2, 3] are known as "bath salts" in the USA, and "plant food" or "research chemicals" in Europe. Synthetic cathinones were made in the 1920's for the medical treatment of parkinsonism, obesity, and depression. Unfortunately, since the beginning of the 21st century, synthetic cathinones have started to be used recreationally with two pioneering representatives: CAT (metcathinone) and 4-MMC (mephedrone, 4-methylmethcathinone), which were followed by methylone (3,4-methylenedioxy-*N*-methylcathinone) and MDPV (3,4-methylenedioxypyrovalerone) [3-5]. New cathinones were synthesized as substitute drugs: butylone, ethylone, buphedrone, and its analog pentedrone, and the constitutional isomer of the latter, 4-MEC (4-methyl-*N*-ethylcathinone), mephedrone derivatives-4-FMC (flephedrone, 4-fluoromethcathinone) and 3-FMC (3-fluoromethcathinone), and α-PVP (α-pyrrolidinopentiophenone) [3, 4, 6].

Considering the potency of cathinones to inhibit dopamine, noradrenaline, and serotonin re-uptake and the ability to liberate these compounds, Simmler et al. [5] classified synthetic cathinones into three groups on the basis of *in vitro* experiments:

1. Cathinones which act like MDMA and cocaine are "*cocaine-MDMA-mixed cathinones*". The mechanism of action of this subgroup of cathinones involves non-selective inhibition of monoamine re-uptake. Representatives of this group are mephedrone, methylone, ethylone, and butylone (similar action to
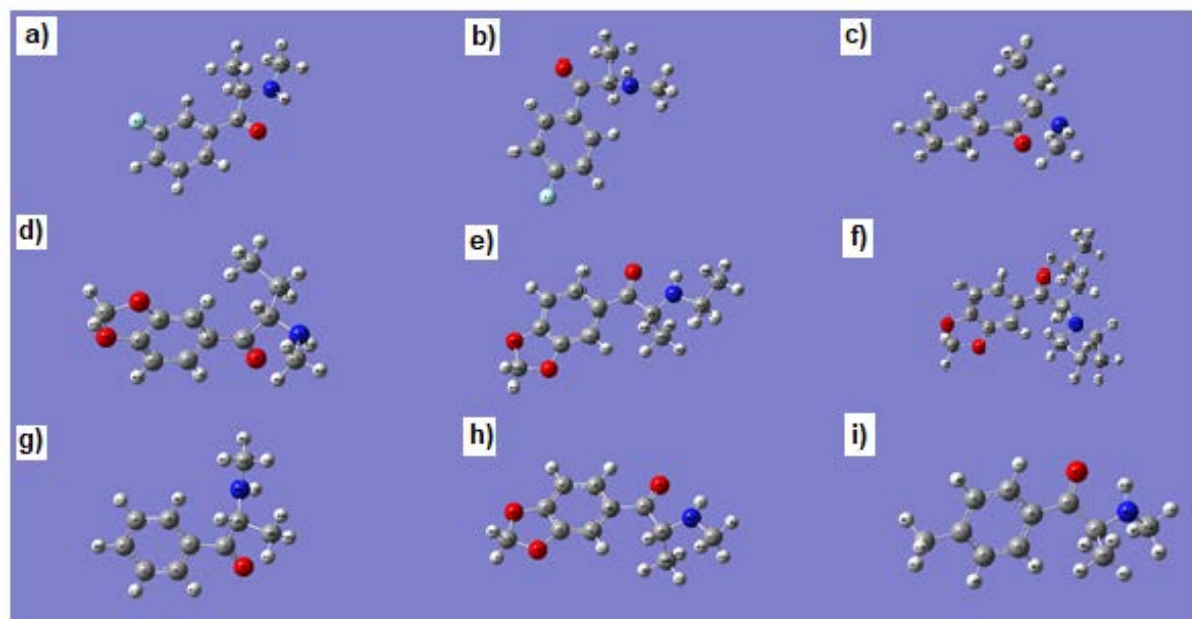
Figure 1: Optimized structures obtained after DFT calculations of a) 3-FMC; b) 4-FMC; c) buphedrone; d) butylone; e) ethylone; f) MDPV; g) metcathinone; h) methylone; i) 4-MMC.

cocaine), and naphyrone (similar action to MDMA) [5, 7-11].

2. Cathinones which act like methamphetamine ("*methamphetamine-like cathinones*"). Their mechanism of action involves the preferential re-uptake inhibition of catecholamines and liberation of dopamine. Methcathinone, flephedrone, and clephedrone (4-chloromethcathinone) belong to this group [5, 7].

3. Synthetic cathinones with structures based on pyrovalerone (*pyrovalerone-cathinones*). The representatives of this group are MDPV and MDPBP, very potent and selective inhibitors of the catecholamine re-uptake demonstrating no neurotransmitter liberating effect [5, 7].

The aim of this study was to perform numerous calculations in order to predict spectra and properties of selected cathinones.

2 Materials and Methods

The selected molecules were treated quantum mechanically by applying DFT method using the Gaussian 09 program suite [12] at the Becke-3-Lee-Yang-Par (B3LYP) level [13, 14] combined with the standard 6-31G basis set. During the optimization procedure all the parameters were set in order to obtain a stable structure with minimum energy. The global minimum energy of the title compound was determined from the structure optimization procedure. The Natural bonding orbital (NBO) analysis was performed using the NBO 5.1 program [15] as implemented in the Gaussian 09 package at DFT/B3LYP level. The hyperconjugation and the interaction energy within the molecule were obtained from the second-order perturbation approach [16-18].

Ethical approval: The conducted research is not related to either human or animal use.

3 Results and discussion

3.1 Molecular geometry

The optimized structures of the title compounds along with numbering of atoms are shown in Figure 1.

The global minimum energy obtained by the DFT structure optimization procedure for the investigated compounds is summarised in Table 1. All the calculated vibrational wavenumbers using the optimized geometry were found to be positive for the title compounds. The bond lengths, bond angles and the optimized parameters calculated using the DFT method are shown in the Supplementary material (Tables A1-A9).

Table 1: Optimized energies of the investigated cathinones.

Drug	Optimized energy (Hartree)
methcathinone	-518.720208
4-MMC	-558.030047
methylone	-707.174321
MDPV	-902.472357
Butylone	-746.478171
Ethylone	-746.481312
buphedrone	-558.024529
4-FMC	-617.934012
3-FMC	-617.932918

In 3-FMC, the bond lengths of C1-C6, C3-C4, C5-C6, C6-C8, C8-C10, C10-C11 were found to be elongated to 1.407 Å, 1.401 Å, 1.409 Å, 1.493 Å, 1.529 Å, 1.562 Å, respectively compared to their default values of 1.39 Å. In the structurally similar 4-FMC, the bond lengths of C1-C6, C5-C6, C6-C8, C8-C10, and C10-C11 were found to be elongated to 1.409 Å, 1.410 Å, 1.489 Å, 1.541 Å, 1.538 Å, respectively, compared to their default values of 1.39 Å. In both cases, C10-H18 and C13-H24 were found to be elongated to 1.1 Å (3-FMC, 4-FMC) and 1.106 Å (3-FMC) and 1.104 Å (4-FMC) compared to their default values of 1.08 Å (3-FMC) and 1.09 Å (4-FMC). This elongation may be due to their proximity to the electronegative oxygen, fluorine and nitrogen atoms [19, 20]. It also indicates the extensive charge delocalization that takes place within the molecule.

In 4-MMC, the bond lengths of C3-C7, C6-C8, C8-C9, and C9-C10 were found to be elongated to 1.506 Å, 1.515 Å, 1.553 Å and 1.524 Å, respectively, compared to their default value of 1.39 Å. Similarly, the bond lengths of C9-H21, C10-H23, and C12-H26 were found to be elongated to 1.097 Å, 1.097 Å and 1.096 Å, respectively, compared to their default value of 1.08 Å. This elongation may be due to their proximity to the electronegative oxygen (O13) and nitrogen (N11) atoms [19, 20] indicating the extensive charge delocalization inside the molecule.

In buphedrone, the bond lengths of C6-C7, C7-C9, C9-C10, and C10-C11 were found to be elongated to 1.518 Å, 1.549 Å, 1.538 Å and 1.52 Å, respectively, compared to their default value of 1.39 Å. The bond lengths of C10-H20, C10-H21, and C13-H26 were found to be elongated to 1.098 Å, 1.099 Å and 1.096 Å, respectively, compared to their default value of 1.08 Å. Our assumption is that the phenomenon is caused by the presence of electronegative oxygen (O8) and nitrogen (N12) atoms [19, 20], which causes the delocalization inside the molecule.

In butylone, the bond lengths of C1-C6, C4-C5, C6-C7, C7-C9, C9-C13, and C13-C14 were found to be elongated to 1.419 Å, 1.401 Å, 1.411 Å, 1.487 Å, 1.545 Å, 1.551 Å and 1.536 Å, respectively, compared to their default value of 1.39 Å. The elongation is observed inside the bonds C13-H24, C14-H26, C16-H30, and C16-H31 as well (1.099 Å, 1.097 Å, 1.105 Å and 1.096 Å, respectively); the default value is 1.08 Å. Electronegative oxygen (O8) and nitrogen (N12) atoms are causes of this elongation and the delocalization of charges inside the molecule [19, 20].

In ethylone, the bond lengths of C6-C7, C7-C9, C9-C13, and C15-C16 were found to be elongated to 1.518 Å, 1.548 Å, 1.529 Å and 1.522 Å, respectively, compared to their default value of 1.39 Å. Similarly, the bond lengths of C11-H21, C11-H22, C13-H24, C13-H25, and C15-H28 were found to be elongated to 1.096 Å, 1.096 Å, 1.096 Å, 1.096 Å and 1.097 Å, respectively from their default value of 1.08 Å. This fact may be due to their proximity to the electronegative oxygen (O8, O10, O12) and nitrogen (N15) atoms [19, 20].

The bond lengths of C1-C6, C4-C5, C5-C6, C6-C7, C7-C9, C9-C10, C10-C19, C16-C17, C17-C18, and C19-C20 in MDPV, were found to be elongated to 1.419 Å, 1.401 Å, 1.412 Å, 1.492 Å, 1.543 Å, 1.546 Å, 1.540 Å, 1.555 Å, 1.534 Å and 1.552 Å and 1.537 Å, respectively (the default value is 1.39 Å). The bond lengths of C9-H24, C10-H26, C15-H30, C16-H32, C19-H37, and C19-H38 were found to be elongated to 1.108 Å, 1.097 Å, 1.108 Å, 1.110 Å, 1.1 Å and 1.099 Å, respectively (the default value is 1.08 Å). The explanation for the elongation and the delocalization can be the presence of electronegative oxygen (O8, O12, O14) and nitrogen (N11) atoms [19, 20]. Regarding Metcathinone, the bond lengths of C1-C6, C2-C3, C3-C4, C5-C6, C6-C7, C7-C9, and C9-C10 were found to be elongated to 1.409 Å, 1.402 Å, 1.4 Å, 1.408 Å, 1.49 Å, 1.541 Å and 1.537 Å, respectively (default value is 1.39 Å). Similarly, the bond lengths of C9-H18, C12-H24, and C12-H25 were found to be elongated to 1.099 Å, 1.104 Å and 1.097 Å, respectively (default value is 1.08 Å). Similarly to previously investigated compounds, electronegative oxygen (O8) and nitrogen (N11) atoms are causes of the observed elongations and delocalisations [19, 20].

The bond lengths of C1-C6, C4-C5, C5-C6, C6-C7, C7-C9, and C9-C10 in the last investigated cathinone here, Methylone, were found to be elongated to 1.419 Å, 1.401 Å, 1.409 Å, 1.486 Å, 1.531 Å and 1.561 Å, respectively (the default value is 1.39 Å). The bond lengths of C9-H19, C10-H20, and C12-H26 were found to be elongated as well (1.099 Å, 1.095 Å and 1.098 Å, respectively) from the default value of 1.08 Å, which can be the consequence of the presence of electronegative oxygen (O8) and nitrogen (N11) atoms [19, 20].

Table 2: Spectral data of the investigated cathinones.

cathinone	UV spectra	FTIR spectra, wavenumbers of the characteristic bands (cm^{-1})	FT Raman spectra, wavenumbers of the characteristic bands (cm^{-1})
methcathinone	239	2708.62; 2454.76; 1691.62; 1597.20; 1469.31; 1360.72; 1244.90; 975.99; 700.19 [23]	1001.5 (v_{12} mode-benzene in-plane ring deformation) [24]
4-MMC	259.5 (257.5) (ethanol) [25] 263.5 (water) [25]	2715.5; 1685.9; 1606.3 [25]	517.9; 637.8 ;804.8; 1248.8; 1605.7 ($v_{8\beta}$ mode) [24]
methylone	Not available	(as hydrochloride): 1676; 1450; 1253; 1091; 740 [26]	589.8; 809.7; 1250.8; 1604.3; 1622.4 [24]
MDPV	233; 282; 315 (methanol) [27]	(as hydrochloride) 2970.26; 2921.23; 2614.76; 1687.17; 1609.53; 1486.95; 1433.83; 1356.19; 1294.94; 1102.84; 1029.28; 935.30; 869.92; 837.23; 743.25; 571.62; 477.64; 428.60 [27]	428.7; 582.5; 716.8; 809.0; 1252.1; 1352.4; 1601.0; 1611.0 [24]
butylone	Not available	1666; 1456; 1253; 1120; 742 [26]	589.0; 720.6; 805.9; 1245.5; 1606.6; 1624.8 [24]
ethylone	Not available	Polymorph A: 1673; 1605; 1556; 1452; 1256; 1038 [28] Polymorph B: 1687; 1613; 1556; 1255; 1035 [28]	Polymorph A: 3079.0; 3036.4; 2991.6; 2950.2; 2937.3; 2900.1; 2891.7; 2803.5; 2748.8; 2705.7; 1672.6; 1620.7; 1607.3; 1558.8; 1509.0; 1447.8; 1428.0; 1404.0; 1363.6; 1299.7; 1286.5; 1250.7; 1217.6; 1209.7; 1176.1; 1137.2; 1119.8; 1090.8; 1045.8; 994.1; 935.8; 908.8; 882.9; 863.1; 826.1; 804.7; 731.0; 720.7; 715.1; 584.1; 521.4; 438.6; 411.5; 383.1; 335.8; 285.9; 238.9; 128.2 [28] Polymorph B: 3070.8; 2987.8; 2977.7; 2932.7; 2882.3; 2802.8; 1685.3; 1613.4; 1604.4; 1571.7; 1555.4; 1505.0; 1463.0; 1453.9; 1437.4; 1412.9; 1381.7; 1351.8; 1298.7; 1287.0; 1271.7; 1253.7; 1232.7; 1204.6; 1177.1; 1148.9; 1107.5; 1084.9; 1038.7; 982.1; 932.1; 860.7; 830.3; 807.6; 735.9; 717.1; 709.2; 577.2; 511.4; 428.0; 413.9; 387.1; 328.8; 257.5; 218.6; 139.7; 119.7; 102.5 [28]
buphedrone	Not available	1681; 1356; 1237; 1117; 760 [29]	Exact values are not available
4-FMC	Not available	2459; 1686; 1594; 1513; 1471; 1410; 1363; 1301; 1238; 1208; 1166; 1113; 1029; 1006; 980; 902; 847; 819; 765; 748; 684 [30]	498.2; 1250.8; 1597.0 [24]
3-FMC	Not available.	2947; 2685; 2439; 1698; 1589; 1478; 1433; 1382; 1364; 1259; 1230; 1218; 1189; 1167; 1096; 1043; 1016; 993; 896; 830; 796; 757; 723; 674 [30]	502.9; 1001.5; 1257.5; 1607.0 [24]

3.2 Molecular vibrations and simulated spectra

The well-known excellent performance of density functional theory for the estimation of vibrational spectra of organic compounds can also be observed for the studied compounds. The unscaled B3LYP/6–31G vibrational wavenumbers are generally somewhat larger than the experimental values. This phenomenon is due to the over-estimation of the basis set and methodology used. However, the use of selective scaling is necessary to obtain reliable information on the vibrational properties. The calculated wavenumbers were scaled using a scale factor [21, 22]. The scaling procedure results in overcoming the anharmonicity and over-estimation. The calculated vibrational wavenumbers, IR intensities, Raman activities along with their assignments for all the title molecules are shown in Tables A10-A18. As shown by the data presented in Table 2 and Tables A10-A18 the theoretical results compare well to the experimental values.

Table 3: Calculated values of quantum chemical parameters of the title molecules.

Chemical parameters	3-FMC	4-FMC	4-MMC	Buphedrone	Butylone	Ethylone	MDPV	Methcathinone	Methylone
E_{HOMO} (eV)	-5.448	-5.973	-5.278	-5.594	-5.599	-5.332	-5.344	-5.803	-5.310
E_{LUMO} (eV)	-2.062	-1.768	-1.644	-1.774	-1.745	-1.697	-1.702	-1.601	-1.699
$\Delta E_{LUMO-HOMO}$ (eV)	3.386	4.205	3.634	3.820	3.854	3.635	3.642	4.202	3.611
Electronegativity (χ)	-3.755	-3.870	3.461	-1.9098	-3.6718	-3.515	-3.5229	-3.3421	-3.504
Pauling Hardness (η)	1.693	2.103	1.8172	1.9098	-1.9268	1.818	1.8209	2.101	1.806
Global Softness (σ)	0.591	0.476	2.9045	2.9289	-0.5189	0.550	0.5492	0.4759	0.554
Global Electrophilicity (ω)	4.164	3.562	10.883	3.4828	-3.4985	3.399	3.4078	2.6581	3.401

3.3 Frontier Molecular Orbital Analysis

The excitation energy of a molecule can be calculated by finding the energy difference between the Highest Occupied Molecular Orbital (HOMO) and the Lowest Unoccupied Molecular Orbital (LUMO), and it is an excellent indicator of electronic transition absorption in the molecular systems [31, 32]. These molecular orbitals provide insight into the reactivity nature and the physical and structural properties of molecules. The positive and negative phase was represented in red and green color. The HOMO, LUMO energies and the energy gap for the investigated compounds were calculated using B3LYP/6-31G method. Owing to the HOMO–LUMO orbital interaction, LP-LP, and LP-bond pair type interactions were observed to be predominant in the investigated compounds according to the molecular orbital theory. The calculated HOMO, LUMO energies, and the energy gap are shown in Table 3.

The molecular orbital analysis for the investigated compounds based on their optimized geometry indicates that the frontier molecular orbitals are mainly composed of p type-atomic orbitals. An electronic system with larger HOMO-LUMO gap should be less reactive than one with a smaller gap. Moreover, the HOMO–LUMO energy gap clearly explains the eventual charge transfer taking place within the molecule.

The power of an electronegative atom in a compound to attract an electron towards it was introduced by Pauling. The parameters such as hardness (η), ionization potential (I), electronegativity (χ), chemical potential (μ), electron affinity (A), global softness (σ) and global electrophilicity (ω) are defined as follows:

$$\chi = -\mu = -\left(\delta E/\delta N \right)_{v(r)} \tag{1}$$

$$I = -E_{HOMO} \tag{2}$$

$$A = -E_{LUMO} \tag{3}$$

$$\chi = (I+A)/2 \tag{4}$$

$$\eta = (I-A)/2 \tag{5}$$

$$\sigma = 1/\eta \tag{6}$$

$$\omega = (\mu^2/2\eta) \tag{7}$$

The ionization energy (IE) can be expressed through HOMO orbital energies, and electron affinity (EA) can be expressed through LUMO orbital energies. The hardness (η) corresponds to the gap between HOMO and LUMO orbital energies. The hardness has been associated with the stability of the chemical system. All the calculated values of quantum chemical parameters of the investigated molecules using the B3LYP method with 6-31G basis set are summarised in Table 3.

From the results in Table 3 it is clear that for the molecules investigated 3-FMC has the minimum energy gap of 3.386 eV and 4-FMC has the maximum energy gap of 4.205 eV. These facts further indicate that 3-FMC would be highly reactive among all the cathinones under investigation.

3.4 Mulliken Population Analysis

The Mulliken population analysis [33, 34] of the title compounds was performed at DFT-B3LYP/6-31G level to obtain the values of the atomic charges and the results are shown in Table 4.

Table 4: Results obtained in Mullikan population analysis.

3-FMC		4-FMC		Butylone		Ethylone		MDPV		Methcathinone		4-MMC		Buphedrone		Methylone	
Atoms	Charges (e)	Atoms	Charges (e)	Atoms	Charges (e)	Atoms	Charges(e)	Atoms	Charges(e)	Atoms	Charges(e)	Atoms	Charges(e)	Atoms	Charges(e)	Atoms	Charges(e)
C1	-0.1468	C1	-0.1105	C1	0.1009	C1	-0.1038	C1	0.0975	C1	0.1304	C1	-0.1325	C1	-0.1419	C1	-0.1038
C2	0.2743	C2	-0.1580	C2	0.2316	C2	0.2319	C2	0.2305	C2	-0.1353	C2	-0.1325	C2	-0.1288	C2	0.2319
C3	-0.1228	C3	0.3012	C3	0.2769	C3	0.2772	C3	0.2770	C3	-0.1082	C3	0.1284	C3	-0.1040	C3	0.2771
C4	-0.1362	C4	-0.1480	C4	-0.1055	C4	-0.1065	C4	-0.1051	C4	-0.1427	C4	-0.1628	C4	-0.1439	C4	-0.1064
C5	-0.1213	C5	-0.1346	C5	-0.1523	C5	-0.1521	C5	-0.1555	C5	-0.1112	C5	-0.1322	C5	-0.1307	C5	-0.1521
C6	0.0375	C6	0.0371	C6	0.0250	C6	0.0280	C6	0.0192	C6	0.0373	C6	0.0427	C6	0.0391	C6	0.0278
F7	-0.3319	F7	-0.3299	C7	0.2863	C7	0.2908	C7	0.2816	C7	0.2999	C7	-0.4764	C7	0.3035	C7	0.2914
C8	0.3005	C8	0.3009	O8	-0.4544	O8	-0.4446	O8	-0.4374	O8	-0.4289	C8	0.2844	O8	-0.4335	O8	-0.4444
O9	-0.4331	O9	-0.4260	C9	-0.0579	C9	-0.0077	C9	0.0066	C9	-0.0511	C9	-0.0642	C9	-0.0759	C9	-0.0075
C10	-0.0095	C10	-0.0552	O10	-0.5480	O10	-0.5484	C10	-0.2298	C10	-0.3936	C10	-0.3638	C10	-0.2206	C10	-0.4117
C11	-0.4122	C11	-0.3921	C11	0.1925	C11	0.1927	N11	-0.4822	N11	-0.5692	N11	-0.5399	C11	-0.4197	N11	-0.5909
N12	-0.5908	N12	-0.5704	O12	-0.5519	O12	-0.5520	O12	-0.5487	C12	-0.2484	C12	-0.2776	N12	-0.5155	C12	-0.2367
C13	-0.2372	C13	-0.2504	C13	-0.2226	C13	-0.4115	C13	0.1930	H13	0.1648	O13	-0.4185	O13	-0.2759	O13	-0.5484
H14	0.1631	H14	0.1720	C14	-0.4211	N14	-0.5964	O14	-0.5524	H14	0.1318	H14	0.1385	H14	0.1679	C14	0.1926
H15	0.1596	H15	0.1539	N15	-0.5349	C15	-0.0717	C15	-0.0790	H15	0.1310	H15	0.1276	H15	0.1345	O15	-0.5521
H16	0.1468	H16	0.1565	C16	-0.2592	C16	-0.4076	C16	-0.0966	H16	0.1291	H16	0.1302	H16	0.1339	H16	0.1619
H17	0.1755	H17	0.1752	H17	0.1630	H17	0.1618	C17	-0.2502	H17	0.1587	H17	0.1680	H17	0.1323	H17	0.1583
H18	0.1418	H18	0.1445	H18	0.1582	H18	0.1582	C18	-0.2865	H18	0.1412	H18	0.1488	H18	0.1399	H18	0.1747
H19	0.1501	H19	0.1529	H19	0.1748	H19	0.1746	C19	-0.2528	H19	0.1538	H19	0.1559	H19	0.1365	H19	0.1386
H20	0.1510	H20	0.1282	H20	0.1269	H20	0.1394	C20	-0.4057	H20	0.1269	H20	0.1639	H20	0.1391	H20	0.1494
H21	0.1378	H21	0.1444	H21	0.1843	H21	0.1837	H21	0.1650	H21	0.1413	H21	0.1272	H21	0.1544	H21	0.1478
H22	0.3070	H22	0.2891	H22	0.1841	H22	0.1843	H22	0.1575	H22	0.2889	H22	0.1437	H22	0.1373	H22	0.1361

Continued **Table 4:** Results obtained in Mullikan population analysis.

3-FMC		4-FMC		Butylone		Ethylone		MDPV		Methcathinone		4-MMC		Buphedrone		Methylone	
Atoms	Charges (e)	Atoms	Charges (e)	Atoms	Charges (e)	Atoms	Charges(e)	Atoms	Charges(e)	Atoms	Charges(e)	Atoms	Charges(e)	Atoms	Charges(e)	Atoms	Charges(e)
H23	0.1456	H23	0.1495	H23	0.1522	H23	0.1483	H23	0.1749	H23	0.1479	H23	0.1539	H23	0.1433	H23	0.3067
H24	0.1138	H24	0.1258	H24	0.1411	H24	0.1493	H24	0.0969	H24	0.1233	H24	0.1260	H24	0.1285	H24	0.1439
H25	0.1370	H25	0.1436	H25	0.1395	H25	0.1358	H25	0.1666	H25	0.1429	H25	0.3128	H25	0.2859	H25	0.1122
				H26	0.1301	H26	0.3017	H26	0.1258			H26	0.1432	H26	0.1461	H26	0.1353
				H27	0.1435	H27	0.1066	H27	0.1834			H27	0.1084	H27	0.1297	H27	0.1838
				H28	0.2892	H28	0.1271	H28	0.1831			H28	0.1370	H28	0.1385	H28	0.1843
				H29	0.1462	H29	0.1278	H29	0.1479								
				H30	0.1225	H30	0.1502	H30	0.1063								
				H31	0.1407	H31	0.1325	H31	0.1561								
								H32	0.1019								
								H33	0.1503								
								H34	0.1259								
								H35	0.1391								
								H36	0.1338								
								H37	0.1190								
								H38	0.1391								
								H39	0.1392								
								H40	0.1292								
								H41	0.1300								

All calculated values indicate the extensive charge delocalization in the investigated molecules [19, 20]. The positive charges are localized over the hydrogen atoms.

3.5 Natural Bond Orbital (NBO) Analysis

The intramolecular interactions, delocalization of electrons and stabilization energy of the investigated compounds was performed with NBO analysis using the NBO 5.1 program [15] implemented in the Gaussian 09W package at the DFT-B3LYP/6-31G level. The energy arising from hyperconjugative interactions was deduced from the second-order perturbation approach [17]. The large values of $E^{(2)}$ indicate the tendency of an electron to donate, and therefore, the greater extent of conjugation within the system.

The strength of the delocalization interaction can be estimated by the second-order energy lowering $E^{(2)}$,

$$E^{(2)} = \Delta E_{ij} = q_i \, F(i,j)^2 \, / \, E_j - E_i \qquad (8)$$

Where $E^{(2)}$ is the stabilization energy, q_i is the donor orbital occupancy, E_i and E_j are the diagonal elements and $F(i,j)$ is the off diagonal NBO Fock matrix element reported [35].

The most predominant electron donor-acceptor interactions are shown in Tables A19-A27 for the investigated compounds.

In 3-FMC, the electron transfer was predominantly observed from the bond pair to bond pairs and lone pair of oxygen and fluorine atoms to bond pairs. A strong hyperconjugative interaction was observed due to π* (C2-C3)--- π* (C4-C5), π* (C8-O9)--- π* (C10-C11), π(C1-C6)--- π*(C2-C3), LP3 (F7)--- π* (C2-C3) and LP2 (O9)--- π* (C6-C8), and values were found to be 159.50 kcal/mol, 97.88 kcal/mol, 22.11 kcal/mol, 17.40 kcal/mol and 17.09 kcal/mol, respectively, which also leads to the stability of the molecule. Although quite similar to 3-FMC, in 4-FMC, the electron transfer was predominantly observed only from the bond pair to bond pairs. A strong hyperconjugative interaction was observed due to π (C1-C6)--- π* (C2-C3), π (C1-C6)--- π* (C4-C5), σ (C1-C2)--- σ* (C2-C3), σ (C1-C2)--- σ* (C6-C8) and σ (C1-C6)--- σ* (C5-C6), and values were found to be 19.27 kcal/mol, 22.11 kcal/mol, 3.97 kcal/mol, 3.37 kcal/mol and 3.82 kcal/mol, respectively.

The electron transfer in 4-MMC was predominantly observed from the bond pair to bond pairs and lone pair of oxygen and nitrogen atoms to bond pairs. A strong hyperconjugative interaction was observed due to π (C$_1$-C$_2$)--- π* (C$_3$-C$_4$), π (C$_1$-C$_2$)--- π* (C$_5$-C$_6$), π* (C$_7$-O$_8$)--- π* (C$_5$-C$_6$), LP (2) O$_8$--- σ* (C$_6$-C$_7$) and LP (2) O$_8$--- σ* (C$_7$-C$_9$). Values were found to be 21.90 kcal/mol, 19.15 kcal/mol, 73.73 kcal/mol, 16.53 kcal/mol and 17.25 kcal/mol, respectively.

In Buphedrone, the electron transfer was predominantly observed from the bond pair to bond pairs and lone pair of oxygen atoms to bond pairs. A strong hyperconjugative interaction was observed due to π* (C$_8$-O$_{13}$)--- π* (C$_1$-C$_6$), π (C$_1$-C$_6$)--- π* (C$_4$-C$_5$), π (C$_1$-C$_6$)--- π* (C$_8$-O$_{13}$), LP (2) O$_{13}$--- σ* (C$_6$-C$_8$) and LP (2) O$_{13}$--- σ* (C$_8$-C$_9$), and the values were 65.53 kcal/mol, 20.09 kcal/mol, 21.33 kcal/mol, 16.55 kcal/mol and 17.01 kcal/mol, respectively.

In Butylone, similarly to 4-MMC, the electron transfer was predominantly observed from the bond pair to bond pairs and lone pair of oxygen and nitrogen atoms to bond pairs. A strong hyperconjugative interaction appeared due to π (C$_3$-C$_4$)--- π* (C$_5$-C$_6$), π (C$_5$-C$_6$)--- π* (C$_1$-C$_2$), π (C$_5$-C$_6$)--- π* (C$_7$-O$_8$), LP (2) O$_{10}$--- π* (C$_3$-C$_4$) and LP (2) O$_{12}$--- π* (C$_1$-C$_2$), and values were found to be 21.41 kcal/mol, 21.38 kcal/mol, 22.06 kcal/mol, 26.68 kcal/mol and 24.92 kcal/mol, respectively.

In Ethylone, similarly to butylone and 4-MMC, the electron transfer was predominantly observed from the bond pair to bond pairs and lone pair of oxygen and nitrogen atoms to bond pairs. A strong hyperconjugative interaction appeared due to π* (C1-C2)--- π* (C5-C6), π* (C3-C4)--- π* (C5-C6), π (C3-C4)--- π* (C5-C6), LP (2)(O12)--- π* (C1-C2) and LP (2)(O10)--- σ* (C3-C4), and values were 228.68 kcal/mol, 229.07 kcal/mol, 20.93 kcal/mol, 25.00 kcal/mol and 26.65 kcal/mol, respectively.

In MDPV (similarly to ethylone, butylone and 4-MMC), the electron transfer was predominantly observed from the bond pair to bond pairs and lone pair of oxygen and nitrogen atoms to bond pairs. A strong hyperconjugative interaction was noticed due to π (C$_1$-C$_2$)--- π* (C$_3$-C$_4$), π (C$_3$-C$_4$)--- π* (C$_5$-C$_6$), π (C$_5$-C$_6$)--- π* (C$_1$-C$_2$), LP (2) O$_{12}$--- π* (C$_3$-C$_4$) and LP (2) O$_{14}$--- π* (C$_1$-C$_2$). Values were found to be 21.12 kcal/mol, 21.02 kcal/mol, 21.44 kcal/mol, 26.57 kcal/mol and 24.74 kcal/mol, respectively.

In Methcathinone, the electron transfer was predominantly observed from the bond pair to bond pairs and lone pair of oxygen and nitrogen atoms to bond pairs. A strong hyperconjugative interaction was due to π (C$_1$-C$_2$)--- π* (C$_3$-C$_4$), π (C$_3$-C$_4$)--- π* (C$_5$-C$_6$), π (C$_5$-C$_6$)--- π* (C$_1$-C$_2$), LP (2) O$_8$--- π* (C$_6$-C$_7$) and LP (1) N$_{11}$--- σ* (C$_9$-C$_{10}$). The energies were found to be 22.07 kcal/mol, 22.30 kcal/mol, 20.55 kcal/mol, 16.38 kcal/mol and 8.48 kcal/mol, respectively.

In Methylone, the electron transfer was predominantly observed from the bond pair to bond pairs and lone pair of oxygen and nitrogen atoms to bond pairs. A strong hyperconjugative interaction was observed due to π (C$_1$-C$_2$)--- π* (C$_3$-C$_4$), π (C$_3$-C$_4$)--- π* (C$_5$-C$_6$), π (C$_5$-C$_6$)--- π* (C$_1$-C$_2$), LP (2) O$_8$--- σ* (C$_6$-C$_7$) and LP (2) O$_{13}$--- π* (C$_3$-C$_4$). The values

Table 5: Thermodynamic parameters of the title compounds computed using DFT/B3LYP/6-31G methodology.

THERMODYNAMIC PARAMETERS	3-FMC	4-FMC	4-MMC	Buphedrone	Butylone	Ethylone	MDPV	Methca-thinone	Methylone
SCF energy (a.u.)	-617.91085	-617.91247	-558.00786	-558.024529	-746.4466	-746.44940	-902.4378	-518.6984	-707.14215
Zero-point Vibrational energy (kcal/mol)	128.68	128.810	151.39073	152.34868	161.600	161.33857	220.3078	134.1173	141.31
Rotational constant (GHz)									
A	1.5066	1.5066	2.08900	1.24361	0.9810	1.32847	0.4538	1.705	1.455
B	0.4254	0.4254	0.37158	0.49817	0.2795	0.22354	0.1930	0.589	0.291
C	0.3561	0.3561	0.33783	0.45433	0.2668	0.20383	0.1626	0.462	0.255
Dipole moment (Debye)									
X	-0.6280	-1.8776	-2.5985	2.2172	-2.8881	2.1312	-2.0092	-0.144	2.121
Y	0.6230	2.1335	-2.4918	0.8253	-1.2119	-2.3338	-1.3365	2.658	-2.304
Z	0.9345	-0.4624	-0.6694	1.8148	0.8815	0.7541	-2.7348	-0.637	0.789
Total	1.2868	2.8794	3.6618	2.9817	3.3257	3.2492	3.6472	2.736	3.230
Total energy									
Energy (kcal/mol)	136.61	136.745	159.949	160.585	171.26	170.992	232.289	141.523	152.13
C_v (cal/mol K)	47.04	46.33	49.725	48.386	57.16	57.369	71.048	43.756	52.64
S (cal/mol K)	111.99	112.783	118.098	116.006	126.990	126.612	148.769	108.494	119.05
Electronic									
Total Energy (kcal/mol)	0.000	0.000	0.000	0.000	0.000	0.000	0.000	0.000	0.000
C_v (cal/mol K)	0.000	0.000	0.000	0.000	0.000	0.000	0.000	0.000	0.000
S (cal/mol K)	0.000	0.000	0.000	0.000	0.000	0.000	0.000	0.000	0.000
Translational									
Total Energy (kcal/mol)	0.889	0.889	0.889	0.889	0.889	0.889	0.889	0.889	0.889
C_v (cal/mol K)	2.981	2.981	2.981	2.981	2.981	2.981	2.981	2.981	2.981
S (cal/mol K)	41.48	41.48	41.422	41.422	42.083	42.083	42.735	41.176	41.88
Rotational									
Total Energy (Kcal/mol)	0.889	0.889	0.889	0.889	0.889	0.889	0.889	0.889	0.889
C_v (cal/mol K)	2.981	2.981	2.981	2.981	2.981	2.981	2.981	2.981	2.981
S (cal/mol K)	31.62	31.60	31.483	31.413	32.752	32.940	34.377	30.916	32.36
Vibrational									
Total Energy (kcal/mol)	134.83	134.967	158.171	158.808	161.48	169.215	230.512	139.745	150.35
C_v (cal/mol K)	41.07	40.87	43.763	42.424	51.20	51.407	65.087	37.795	46.67
S (cal/mol K)	38.98	39.68	45.193	43.171	52.15	51.589	71.656	36.402	44.80

were found to be 20.88 kcal/mol, 20.93 kcal/mol, 21.33 kcal/mol, 16.76 kcal/mol and 26.64 kcal/mol, respectively.

3.6 Thermodynamic Parameters

The thermodynamic parameters, namely, heat capacity, entropy, rotational constants, dipole moments, vibrational zero-point energies, of the molecules under investigation have also been computed at DFT-B3LYP level using 6-31G basis set and are presented in Table 5. The thermodynamic data provides useful information for further studies of the investigated compounds [36]. These standard thermodynamic functions can be used as reference thermodynamic values to calculate changes of entropies (ΔS_T), changes of enthalpies (ΔH_T) and changes of Gibbs free energies (ΔG_T) of the reaction. The dipole moment and its principal inertial axes are strongly dependent upon the conformation of the molecule.

4 Conclusions

The use of DFT calculations has been shown to be a useful method for predicting vibrational and infra-red spectra of selected cathinones, particularly using the appropriate scaling. Therefore, this method can be used to predict the spectra of newly synthesized and not fully characterised cathinones which would be useful in forensics.

References

[1] Chung H, Lee J, Kim E. Trends of novel psychoactive substances (NPSs) and their fatal cases. Forensic Toxicol. 2016;34(1):1–11.

[2] Kelly JP. Cathinone derivatives: a review of their chemistry, pharmacology and toxicology. Drug Test Anal. 2011 Jul-Aug;3(7-8):439–53.

[3] Zawilska JB, Wojcieszak J. Designer cathinones—an emerging class of novel recreational drugs. Forensic Sci Int. 2013 Sep;231(1-3):42–53.

[4] Valente MJ, Guedes de Pinho P, de Lourdes Bastos M, Carvalho F, Carvalho M. Khat and synthetic cathinones: a review. Arch Toxicol. 2014 Jan;88(1):15–45.

[5] Simmler LD, Buser TA, Donzelli M, Schramm Y, Dieu LH, Huwyler J, et al. Pharmacological characterization of designer cathinones in vitro. Br J Pharmacol. 2013 Jan;168(2):458–70.

[6] Katz DP, Bhattacharya D, Bhattacharya S, Deruiter J, Clark CR, Suppiramaniam V, et al. Synthetic cathinones: "a khat and mouse game". Toxicol Lett. 2014 Sep;229(2):349–56.

[7] Baumann MH, Ayestas MA Jr, Partilla JS, Sink JR, Shulgin AT, Daley PF, et al. The designer methcathinone analogs, mephedrone and methylone, are substrates for monoamine transporters in brain tissue. Neuropsychopharmacology. 2012 Apr;37(5):1192–203.

[8] López-Arnau R, Martínez-Clemente J, Pubill D, Escubedo E, Camarasa J. Comparative neuropharmacology of three psychostimulant cathinone derivatives: butylone, mephedrone and methylone. Br J Pharmacol. 2012 Sep;167(2):407–20.

[9] Martínez-Clemente J, Escubedo E, Pubill D, Camarasa J. Interaction of mephedrone with dopamine and serotonin targets in rats. Eur Neuropsychopharmacol. 2012 Mar;22(3):231–6.

[10] Meyer MR, Wilhelm J, Peters FT, Maurer HH. Beta-keto amphetamines: studies on the metabolism of the designer drug mephedrone and toxicological detection of mephedrone, butylone, and methylone in urine using gas chromatography-mass spectrometry. Anal Bioanal Chem. 2010 Jun;397(3):1225–33.

[11] Dargan PI, Sedefov R, Gallegos A, Wood DM. The pharmacology and toxicology of the synthetic cathinone mephedrone (4-methylmethcathinone). Drug Test Anal. 2011 Jul-Aug;3(7-8):454–63.

[12] Frisch MJ, Trucks GW, Schlegel HB, Scuseria GE, Robb MA, Cheeseman JR, et al. Gaussian 09, Revision D.01. Wallingford (CT): Gaussian Inc.; 2009.

[13] Becke AD. Density-functional thermochemistry. III. The role of exact exchange, J Chem Phys. 1993;98:5648e5652.

[14] Lee C, Yang W, Parr RG. Development of the Colle-Salvetti correlation-energy formula into a functional of the electron density. Phys Rev B.1988;37:785e789.

[15] Glendening ED, Badenhoop JK, Reed AE, Carpenter JE, Bohmann JA, Morales CM, et al. NBO 5.0, Theoretical Chemistry Institute, University of Wisconsin, Madison; 2001.

[16] Weinhold F., Chemistry: a new twist on molecular shape, Nature, 2001, 411, 539e541.

[17] Li XH, Zhang RZ, Zhang XZ. Natural bond orbital analysis of some parasubstituted *N*-nitrosoacetanilide biological molecules. Struct Chem. 2009;20(6):1049–54.

[18] Reed AE, Curtiss LA, Weinhold F. Intermolecular interactions from a natural bond orbital, donor-acceptor viewpoint. Chem Rev. 1988;88:899e926.

[19] Bondi A. van der Waals volumes and radii of metals in covalent compounds. J Phys Chem A. 1966;70(9):3006–7.

[20] Klein RA. Modified van der Waals atomic radii for hydrogen bonding based on electron density topology. Chem Phys Lett. 2006;425(1-3):128–33.

[21] Rauhut G, Pulay P. Transferable scaling factors for density functional derived vibrational force fields. J Phys Chem. 1995;99:3093e3100.

[22] NIST Computational Chemistry Comparison and Benchmark Database, NIST Standard Reference Database Number 101, Release 19, April 2018, Editor: Russell D. Johnson III; 2018 http://cccbdb.nist.gov/

[23] http://www.swgdrug.org/Monographs/METHCATHINONE.pdf, accessed 6 August 2019

[24] Christie R, Horan E, Fox J, O'Donnell C, Byrne HJ, McDermott S, et al. Discrimination of cathinone regioisomers, sold as 'legal highs', by Raman spectroscopy. Drug Test Anal. 2014 Jul-Aug;6(7-8):651–7.

[25] Santali EY, Cadogan AK, Daeid NN, Savage KA, Sutcliffe OB. Synthesis, full chemical characterisation and development of validated methods for the quantification of (±)-4′-methylmethcathinone (mephedrone): a new "legal high". J Pharm Biomed Anal. 2011 Sep;56(2):246–55.

[26] Maheux CR, Copeland CR, Pollard MM. Characterization of three methcathinone analogs: 4-methylmethcathinone, methylone, and bk-MBDB. Microgram J. 2010;7(2):42–9.

[27] Yohannan JC, Bozenko JS Jr. The characterization of 3,4-methylenedioxypyrovalerone (MDPV). Microgram J. 2010;7(1):12–5.

[28] Maheux CR, Alarcon IQ, Copeland CR, Cameron TS, Linden A, Grossert JS. Identification of polymorphism in ethylone hydrochloride: synthesis and characterization. Drug Test Anal. 2015.

[29] Maheux CR, Copeland CR. Chemical analysis of two new designer drugs: buphedrone and pentedrone. Drug Test Anal. 2012 Jan;4(1):17–23.

[30] Archer RP. Fluoromethcathinone, a new substance of abuse. Forensic Sci Int. 2009 Mar;185(1-3):10–20.

[31] Dolbier Jr. WR, Burkholder CR. Diels-Alder reactions of fluoroallene. An affirmation of homo-lumo control. Tetrahedron Lett. 1980;21:785e786.

[32] Wolfe S, Livneh M, Cohen D, Hoz S. The ambident nucleophilic center. Stereochemical consequences of HOMO-LUMO and HOMO-HOMO dominant processes. Isr J Chem. 1989;29:221e227.

[33] Mulliken RS. A new electroaffinity scale; together with data on valence states and on valence ionization potentials and electron affinities. J Chem Phys. 1934;2(11):782–95.

[34] Mulliken RS. Electronic structures of molecules XI. Electroaffinity, molecular orbitals and dipole moments. J Chem Phys. 1935;3(9):573–85.

[35] Ragavendran V, Muthunatesan S. New insights into the vibrational spectroscopic investigation on S-cis & S-trans forms of 2-Methoxy benzoyl chloride. Vib. Spec. 2017;92:35–45.

[36] Ragavendran V, Muthunatesan S. An insight into the conformational flexibility and vibrational behavior of 2-nitroso-1-naphthol: A density functional theory approach. Spectrosc Lett. 2016;49(4):294–303.